WARSAW UNIVERSITY OF TECHNOLOGY Index 351733
FACULTY OF CIVIL ENGINEERING
COMMITTEE FOR CIVIL AND WATER ENGINEERING
POLISH ACADEMY OF SCIENCES ISSN 1230-2945

DOI: 10.24425/ace.2025.154110

ARCHIVES OF CIVIL ENGINEERING

Vol. LXXI ISSUE 2 2025

pp. 99–112

Research paper

Digital landscape architecture design using high resolution remote sensing image interpretation

Hang Yin[1], Lanyu Chang[2], Guangpeng Yue[3]

Abstract: With the continuous development of remote sensing technology and the widespread application of high-resolution remote sensing images, digital landscape design based on high-resolution remote sensing image interpretation is gradually becoming a new design concept and method. This study is based on high-resolution remote sensing images to classify gardens, and combined with ground survey data, statistical analysis software is used to invert the landscape elements of gardens. The experimental results showed that the R^2 value was relatively large, while the MRE and RMSE values were small, indicating that the analysis results were close to the true values and the fitting effect was relatively ideal. The overall image segmentation was excellent, with an average diameter at breast height of 8.0–17.0 cm, mixing degree of 0.4–0.6, vertical diversity of 0.5–0.8, and a clear forest hierarchy when the average density was between 800–1100 plants/hm^2. This indicates that the quality of landscape architecture designed at this landscape scale changes significantly and the effect is good. Digital landscape design based on high-resolution remote sensing image interpretation can not only improve design efficiency and accuracy, but also provide strong support for the sustainable development of urban planning and landscape design.

Keywords: high-resolution remote sensing, digital landscape architecture, planning and design, forest stand structure

[1]Prof., MSc., Luxun Academy of Fine Arts, College of Architectural Art Design, 110000 Shenyang, China, e-mail: yinhang810508@163.com, ORCID: 0009-0005-9949-8308

[2]MSc., Luxun Academy of Fine Arts, Experimental Art Department, 110000 Shenyang, China, e-mail: 15242465559@163.com, ORCID: 0009-0005-5449-4776

[3]Prof., MSc., Luxun Academy of Fine Arts, College of Industrial Design, 110000 Shenyang, China, e-mail: ygp6820620@163.com, ORCID: 0009-0002-6574-5727

1. Introduction

Landscape architecture is an art form established in nature. In landscape design, emphasis is placed on organically integrating natural and cultural factors to create a garden environment rich in emotions and beauty [1]. Digital landscape design is one of the popular research directions in the field of urban planning and landscape design. With the continuous development of remote sensing technology (RS) and the widespread application of high-resolution remote sensing images (RSI), the use of high-resolution RSI interpretation in digital landscape design is gradually becoming a new design concept and method [2]. This design method can more accurately capture and simulate the characteristics of the natural environment by analyzing and interpreting the surface information in RSIs, providing a large amount of accurate geographic data, and providing new means and tools for the planning, design, and management of landscape architecture [3, 4]. At the same time, high-resolution RSIs can also be assisted by RS technology to evaluate and optimize landscape design schemes, improving the feasibility and effectiveness of design schemes, and achieving deep understanding and simulation of the natural environment [5]. However, to achieve effective application of this design method, there are still some challenges and difficulties, such as data acquisition and processing, algorithm research, and technological applications. Therefore, further in-depth research and exploration are needed to promote the development of digital landscape design and make greater contributions to urban construction and environmental protection. The aim of this study is to investigate the design methods of digital landscape architecture through the application of high-resolution RSI interpretation technology. Taking the planning and design of landscape architecture as the research object, high-resolution RSI interpretation technology is used to interpret the planning scheme.

The research content is divided into four parts: The second part provides an overview of the current research status of digital landscape design based on high-resolution RSI interpretation. The third part proposes a high-resolution RSI classification and information extraction method, which is combined with landscape element extraction. The fourth part conducts experimental verification on the constructed landscape architecture model and analyzes the experimental results.

2. Literature

At present, the spatial feature division of landscape patterns is mainly based on methods such as RSIs and dynamic research. Liu proposed a landscape pattern partitioning method using multi-source RS technology by combining information entropy and grid partitioning to extract spatial distribution characteristics of landscape patterns. Results showed that the method designed for the study only took 0.22 minutes to extract the spatial distribution features of landscape patterns [6]. Li et al. proposed a landscape image feature extraction and image retrieval method using image processing to address the issue of landscape image retrieval and management in landscape digital image libraries. Results showed that the proposed method improved the retrieval performance of landscape images [7]. Dong et al. proposed a sustainable landscape model (SLP) using spatial planning systems, which constructed a stable ecosystem

service based on ecological networks and ecological security patterns. The results indicated that SLP effectively supported spatial planning and was applied to future ecosystem construction [8]. Fu F. et al. used the CA Markov model to predict and simulate the landscape pattern, and the simulation results showed that over time, the building and water area significantly increased [9].

RS is a comprehensive ground to ground observation method that emerged in the early 21st century, can quickly obtain large-scale, multi temporal, and multi-band land information. In the process of structural division and feature extraction in the above-mentioned landscape architecture, using RS technology to divide the landscape pattern can improve the efficiency of feature extraction, but there are still some problems that need to be expanded in many aspects. Świerkosz et al. proposed a landscape quality indicator analysis method using RS data to address the issue of landscape quality assessment. The results indicated that the proposed method had advantages in landscape quality assessment and can be used to classify protected areas [10]. Miller et al. proposed an efficient data collection method that removes GCP to address the issue of imprecision in unmanned aerial RS platform data. The results indicated that unmanned aerial systems saved time and provided high-precision data with resolutions lower than decimeters [11]. Mulverhill et al. evaluated the consistency of forest canopy products and terrestrial ecosystem monitoring systems in forest regeneration areas based on RS data. The results indicated that the simulated altitude based on optical satellite RS data had less generalized distribution than the altitude of Landsat 2 [12].

In summary, the changes in landscape appearance lead to different visual effects. At present, further research is needed to obtain the above landscape information through RS methods, including RSI interpretation methods, landscape patch classification, and ground validation. Therefore, this study uses high-resolution RSIs and ground survey data for classification to study the impact of landscape elements such as stand spatial structure, stand density, tree species composition, and forest spatial pattern on landscape RS interpretation of scenic forests.

3. Method

This study first classifies scenic gardens based on high-resolution RSIs. Based on RS classification, the structural status of various scenic forests in the experimental area is analyzed. Then, statistical analysis software is used to simulate landscape elements such as tree species composition, stand density, stand spatial structure, forest spatial pattern, and canopy structure of scenic forests in the experimental area, analyzing the impact of landscape elements on forest spatial pattern.

3.1. Classification and information extraction of high resolution RSIs

A very important aspect of digital landscape design is to accurately capture and simulate the characteristics of the natural environment, so there is a close relationship between landscape architecture and high-resolution RS. High resolution RSIs can provide detailed geographic information, terrain data, and visual support for various stages of landscape architecture design,

thereby providing basic data for design, improving design quality and construction efficiency. This study utilizes high-resolution RSIs to interpret and analyze RSI data. The overall technical roadmap is shown below.

From Fig. 1, it can be seen that the main technical route of the study is divided into two routes: one is the processing of RS data, and the other is the investigation of sample plots. Satellite remote sensors can obtain ground information by collecting the position of ground targets, reflecting sunlight, and radiating far-infrared radiation [13]. In order to obtain clear images, geometric accuracy correction and spatial registration must first be performed. By selecting easily recognizable ground control points within the image range and using GPS field deployment, geometric distortions caused by RSIs are corrected. Due to the differences in target features between RSIs and reference systems, the original image has deformation errors, while the objective of orthophoto images is to eliminate geometric distortions [14]. Selecting ground control points through GPS deployment and generating a Digital Elevation Model (DEM) for fusion with multispectral images can obtain spectral data containing both high-resolution and multispectral information. Applying Gaussian universal filtering can process panchromatic images, removing useless information [15]. Using multi-scale image segmentation methods to segment image scan obtain tree species information [16]. Before image segmentation, the spectral factor and shape factor are determined, where the shape factor includes smoothness heterogeneity and compactness heterogeneity. The calculation method for heterogeneity is shown in Equation (3.1).

$$\begin{cases} H = wh_c + (1-w) \cdot h_s \\ w_c + w_s = 1 \end{cases} \tag{3.1}$$

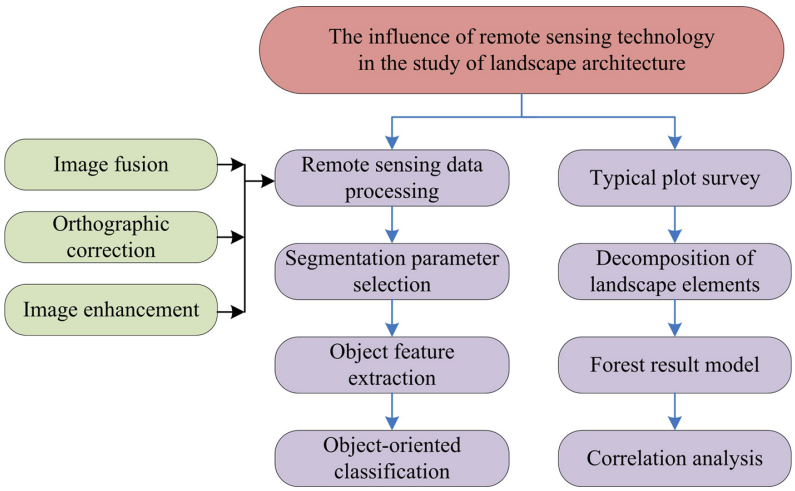

Fig. 1. Schematic diagram of the overall technical route of the research

In Equation (3.1), H represents the heterogeneity of the image, w represents user-defined weights, with a range of values between [0, 1], w_c represents spectral weights, and w_s represents shape weights. h_c and h_s represent spectral heterogeneity and shape heterogeneity.

The calculation method of h_c is shown in Equation (3.2).

$$h_c = \sum w_c \left(n_m \cdot \sigma_c^m - \left(n_o \cdot \sigma_c + n_o \cdot \sigma_c^o\right)\right) \tag{3.2}$$

In Equation (3.2), n represents the number of pixels in the image,n_m represents the number of merged pixels, n_o represents the number of phase elements of the object, and σ_c represents the standard deviation of internal pixel values. On the other hand, the calculation method for h_s shape heterogeneity is shown in Equation (3.3).

$$h_s = w_c \cdot h_c + (1 - w_c) \cdot h_s \tag{3.3}$$

In Equation (3.3), h_s shape heterogeneity is related toshape compactness and shape smoothness. To minimize the average heterogeneity of various objects in an image, it is necessary to ensure that smoothness heterogeneity, spectral heterogeneity, and compactness are minimized [17, 18]. According to the information content of each band, the standard deviation of image homogeneity is shown in Equation (3.4).

$$\sigma_L = \sqrt{\frac{1}{n-1}\sum_{i=1}^{n}(C_{Li} - C_L)^2} \tag{3.4}$$

In Equation (3.4), L represents a single band, σ_L represents the standard deviation of image homogeneity, C_L represents the mean grayscale within the image, and C_{Li} represents the grayscale value of pixel i. The method for calculating the heterogeneity of any segmented image is shown in Equation (3.5).

$$\Delta C_L = \frac{1}{l}\sum_{i=1}^{t} l_i \left|C_L - C_{Li}\right| \tag{3.5}$$

In Equation (3.5), l represents the boundary length of the image, t represents the number of adjacent images of the current object, and l_i represents the length of the common edge with the i-th adjacent object. The segmentation evaluation index of the image is constructed according to Equations (3.4) and (3.5), and the segmentation evaluation index is calculated in Equation (3.6).

$$\mathrm{SEI}_L = \frac{\Delta C_L}{\sigma_L} \tag{3.6}$$

In Equation (3.6), SEI represents the segmentation evaluation index of the image. When encountering multi band situations, SEI is modified to Equation (3.7).

$$\mathrm{SEI} = \sum_{L=1}^{m} w_L \cdot \mathrm{SEI}_L \tag{3.7}$$

The average SEI values of each target are taken to compare the images at different segmentation scales [19]. The average segmentation evaluation index is shown in Equation (3.8).

$$\mathrm{ASEI} = \frac{1}{A}\sum_{i=1}^{n} A_i \cdot \mathrm{SEI}_i \tag{3.8}$$

In Equation (3.8), A represents the total area of all images, A_i represents the area of the i-th image, SEI_i represents the SEI of the i-th image, and ASEI represents the average segmentation evaluation index of the image.

3.2. Extraction and design of landscape element information in digital landscape architecture

The digital landscape garden designed for this study is located in Baishan City, Jilin Province, and belongs to the continental monsoon climate of the northern temperate zone. The landscape architecture studied mainly consists of tree species such as red spruce, poplar, birch, sand pine, and mixed coniferous and broad-leaved forests. The satellite RSI data obtained using GF7 satellite is studied, investigates forest structural parameters related to the aesthetic quality of scenic forests. Among them, the spatial structure of forest stands is crucial for tree growth, as it reflects the spatial distribution and relationships of species within forest communities [20, 21]. The study used GF7 satellite to obtain satellite RSI data and investigated forest structural parameters related to the aesthetic quality of scenic forests. The degree of mixing is calculated in Equation (3.9).

$$M = \frac{n_s}{N} \cdot \frac{m}{M} \cdot \frac{q}{M} \tag{3.9}$$

In Equation (3.9), q represents the total number of non-repetitive neighboring connection relationships, m represents the number of neighboring heterogeneous connection relationships, M represents the total number of adjacent individual connection relationships, N represents the total number of individuals, and n_s represents the number of species. According to Equation (3.9), the calculation method for the average mixing degree of multiple points is shown in Equation (3.10).

$$\overline{M} = \frac{1}{K} \sum_{i=1}^{k} M_i \tag{3.10}$$

In Equation (3.10), $\overline{M}$ represents the average mixing degree at multiple points, M_i represents the mixing degree at point i, and K represents the number of tree species in the average mixing degree at multiple points. The radial dispersion of different forest spatial structures D is calculated in Equation (3.11).

$$D = \frac{D_{\max} - D_{\min}}{D_{\text{mean}}} \tag{3.11}$$

In Equation (3.11), D_{mean} represents the average diameter of the forest stand, $D_{\min}$ represents the minimum diameter of the forest stand, and $D_{\max}$ represents the maximum diameter of the forest stand. The vertical hierarchy of the stand is represented by the vertical diversity index Z, which is calculated using the Equation (3.12).

$$Z = -\sum_{i=1}^{n} P_i In\left(P_i\right) \tag{3.12}$$

In Equation (3.12), P_i represents the proportion of height at a certain level in the total height of the forest stand. Through inversion in the experimental area, the relationship between forest structure of ground landscape types and RSI interpretation information is analyzed. The stepwise regression is a method for selecting the optimal regression equation, and its process is shown in Fig. 2.

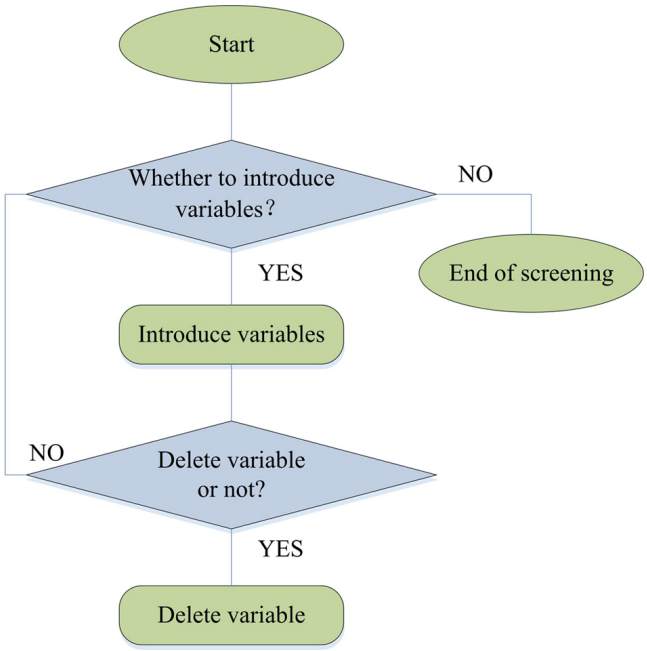

Fig. 2. Stepwise regression flowchart

To test the accuracy, test criteria such as coefficient of determination, mean relative error, and total root mean square error are used to select the optimal prediction model and parameters. The coefficient of determination measures the correlation between the independent and dependent variables and the quality of the regression results. Its calculation method is shown in Equation (3.13).

$$R^2 = 1 - \frac{\sum_{i=1}^{n} \left(y_i - \widehat{y}_i\right)^2}{\sum_{i=1}^{n} \left(y_i - \overline{y}_i\right)^2}. \tag{3.13}$$

In Equation (3.13), R^2 represents the coefficient of determination,n represents the number of samples, $\overline{y}_i$ represents the average value, y_i represents the measured value, and $\widehat{\rightarrow}\ y_i$ represents the predicted value. The average relative error of the inspection standard is calculated in Equation (3.14).

$$\mathrm{MRE} = \frac{1}{n} \sum_{i=1}^{n} \left| \frac{y_i - \widehat{y}_i}{y_i} \right| \times 100\% \tag{3.14}$$

In Equation (3.14), MRE represents the average relative error, the larger the value MRE. The root mean square difference of the inspection standard is calculated in Equation (3.15).

$$\text{RMSE} = \sqrt{\frac{\sum_{i=1}^{n}\left(y_i - \widehat{y}_i\right)^2}{n}} \tag{3.15}$$

In Equation (3.15), RMSE represents the total root mean square difference. In summary, this study adopts object-oriented technology to classify remote sensing images and provide reliable basis for digital landscape design.

4. Experimental results

4.1. Performance evaluation of remote sensing image segmentation

A study on digital assisted design was conducted in a scenic garden area in Baishan City. The satellite RSI data obtained was studied using GF7 satellite and process landscape data using ArcGIS and SPSS software. With the GF7 satellite RSI data, the 1985 National Altitude Datum was used, with WGS84 coordinates as the geodetic reference. The 2022 forest resource planning survey of the experimental area was the basic map. Based on the terrain and forest pattern characteristics of the scenic gardens, GPS positioning was used for each sample plot, with a sample plot area of 400 m^2 or 900 m^2. The optimal segmentation scale parameters for residential areas, main roads, water bodies, and forests were respectively the optimal segmentation scale parameters for each region, as shown in Table 1.

Table 1. Optimal multi-scale segmentation parameters

Extracting information	Segmentation layer	Segmentation scale	Colour	Shape	Smoothness	Compactness
Forest	Level 1	140	0.9	0.1	0.5	0.5
Water	Level 2	110	0.7	0.3	0.6	0.4
Main road	Level 3	70	0.7	0.3	0.6	0.4
Building	Level 4	40	0.8	0.2	0.6	0.4

Based on the characteristics of RSIs of landscape architecture, a visual interpretation method was adopted to extract terrain information from GF7 satellite RSIs. Based on RSIs, the study selected some land feature categories with clear ground boundaries and easy to distinguish for image segmentation performance evaluation. The results are shown in Fig. 3.

From Fig. 3, it can be seen that among various evaluation indicators, the evaluation values of water bodies were relatively low. In the roundness evaluation index, the average value of the road was the lowest, indicating good segmentation effect. The reason may be that the road had regularity and a single shape. In the evaluation indicators of shape factor and area error, the

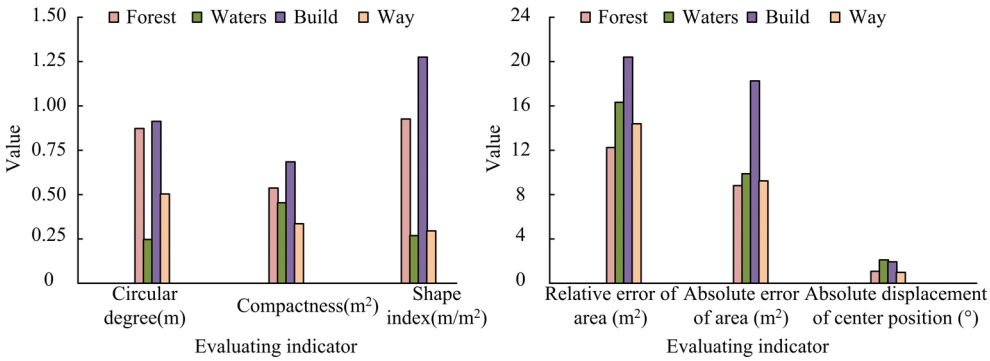

Fig. 3. Evaluation of image segmentation effect

evaluation value of buildings was relatively high, which may be due to the uneven shape and scattered distribution of buildings in landscape architecture on satellite RSIs. The absolute displacement of the central positions of forests, water bodies, roads, and buildings was around two degrees, indicating that the control points selected for the reference and segmentation objects were close.

4.2. Performance evaluation of remote sensing image classification

In order to achieve a more detailed analysis, it was necessary to further classify and segment the forest land. This study was based on previously classified images and used supervised classification methods to perform a second segmentation of forests. By summarizing the overall classification accuracy and coefficients based on ground survey sample information, smaller scale and higher homogeneity images were obtained for more detailed analysis. To study the spatial structure of forest stands in landscape architecture, experiments were conducted using density, dispersion, mixing angle, and vertical diversity as indicators. The results are shown in Fig. 4.

From Fig. 4(a), it can be seen that tree species with a diameter dispersion greater than 1 indicated significant differentiation within the forest stand, while those with a diameter dispersion less than 1 were mostly tree species in the juvenile stage. In Fig. 4(b), the mixing degree of tree species such as spruce, red pine, and larch was all below 0.4, while the mixing degree of broad-leaved mixed forests was around 0.7. The reason may be that broad-leaved mixed forests had multiple tree types, random and complex dispersion, and rich color changes. In Fig. 4(c), the vertical diversity values of broad-leaved mixed forests were relatively high, indicating that the internal structure of broad-leaved mixed forests was complex and diverse. In Fig. 4(d), the stand height difference of broad-leaved mixed forest and Korean pine forest was both greater than 10 m, and most of the other tree species were also between 6–9 m, indicating that the overall distribution of the forest in the study area had a sense of hierarchy, and the distribution of tree species was staggered. To test the accuracy, statistical analysis software was used for data analysis, with diameter dispersion, mixing degree, vertical diversity, and stand density as dependent variables. Test criteria such as coefficient of determination, mean relative error, and total root mean square difference were used for testing. The results are shown in Fig. 5.

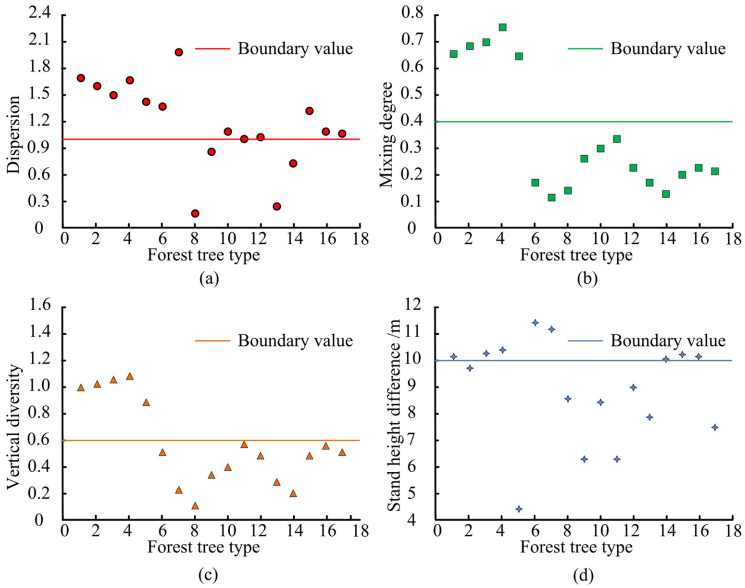

Fig. 4. Spatial structure of forest stands in the study area; (a) Dispersion of different trees, (b) Mixed degree of different trees, (c) Vertical diversity of different trees, (d) Stand height difference of different trees

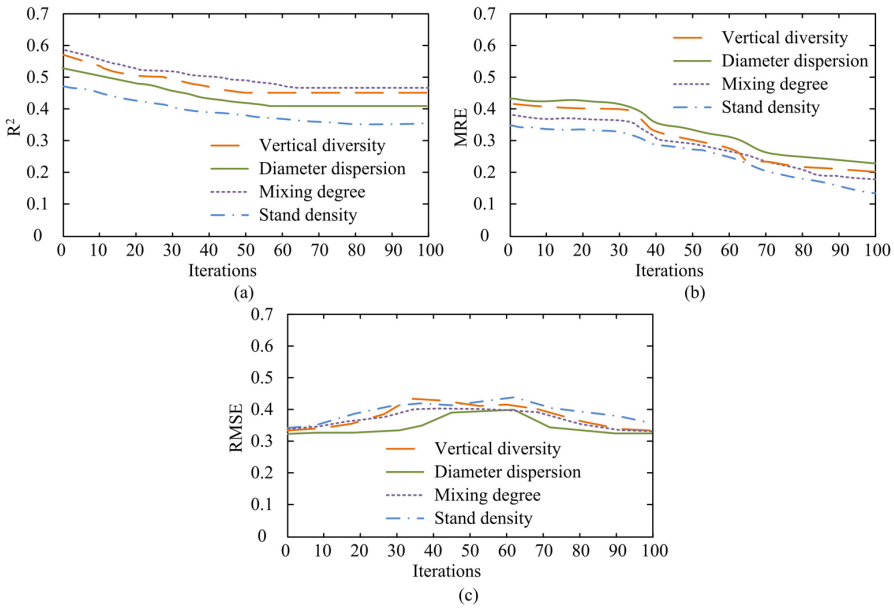

Fig. 5. Precision inspection results; (a) R^2 test results, (b) MRE test results, (c) RMSE test results

In Fig. 5, during the accuracy test of the study area, the R^2 value of the mixing degree in Fig. 5(a) was the highest, around 0.55. The larger the R^2 value, the better the regression prediction effect. From Fig. 5(b) and 5(c), the values of MRE and RMSE were both between 0.3 and 0.5, which were relatively small, indicating that the analysis results were close to the true values and the fitting effect was relatively ideal. By using the single factor clustering function of the software, forest structural parameters with significant impact were graded, and the differences in the impact of structural parameters on RS classification accuracy at different levels were analyzed in detail in Fig. 6.

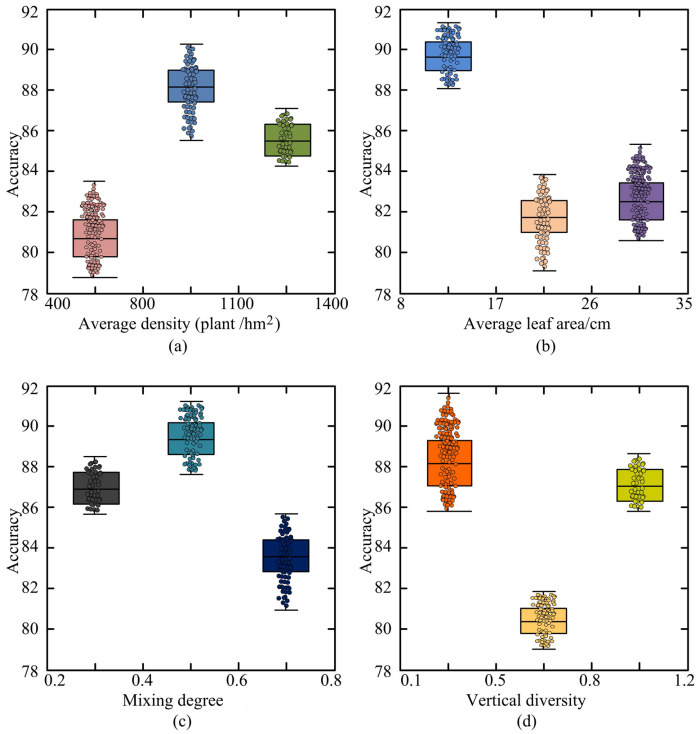

Fig. 6. The impact of forest structure factors on RS classification accuracy; (a) Influence of average density on classification accuracy of remote sensing, (b) Influence of mean DBH on classification accuracy of remote sensing, (c) Influence of mixing degree on classification accuracy of remote sensing, (d) Influence of vertical diversity on classification accuracy of remote sensing

From Fig. 6, it can be seen that when the average diameter at breast height was between 8.0–17.0 cm, the degree of mixing was 0.4–0.6, the vertical diversity was 0.5–0.8, and the average density was between 800–1100 plants/hm^2, the impact on the classification accuracy of RSIs was the lowest. The scenic forest area was characterized by large diameter and complex mixed degree, with obvious forest stand hierarchy at medium density. The quality of landscape gardens designed at this landscape scale changed significantly, and the effect was good. To further validate the remote sensing image classification performance of this research method,

the Trento dataset containing 30214 ground truth samples was used for experiments. The Trento dataset consists of 6 categories, and this study selected four categories from the dataset: Buildings, Apple trees, Ground, and Vineyard for testing. And compared with convolutional neural networks (CNN), adversarial learning classification networks (ALNet), and encoder decoder based classification networks (EDNet). The classification accuracy of the four image classification methods is shown in Fig. 7.

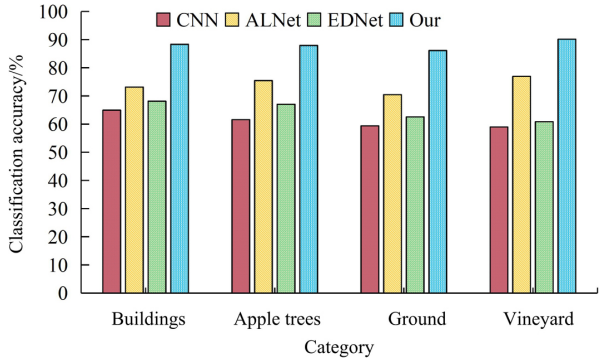

Fig. 7. Classification accuracy of four image classification methods

From Fig. 7, it can be seen that the classification accuracy of our research method is consistently the highest among the four categories of Buildings, Apple trees, Ground, and Vineyard, with values of 88.34%, 87.92%, 86.13%, and 90.14%, respectively, demonstrating good image classification performance. Next is ALNet, with CNN performing the worst.

5. Conclusions

Aiming at the problem of extracting and identifying landscape elements of landscape forest in digital landscape architecture design, this study classifies landscape remote sensing images of landscape forest based on high-resolution remote sensing image interpretation to explore the influence of different landscape scales on landscape architecture. The results show that the evaluation value of water area in image segmentation is relatively low because of its spectral uniqueness. This reflects the high recognition degree of water features in remote sensing images. However, due to its regularity and shape, the average value of roundness evaluation index of roads is low, which reflects the good effect of road identification and segmentation in remote sensing images. In contrast, buildings are characterized by different shapes and sizes and scattered distribution in landscape architecture, so the evaluation value of shape factor and area error evaluation index is larger. This reveals the difficulty and challenge of segmentation when dealing with complex structures. For the further classification and segmentation of forest land, a smaller segmentation scale is adopted to cope with the complexity of forest land structure and the characteristics of large patch area. Through supervised classification method, based on the information of ground survey sample plots, the overall classification accuracy and

coefficient are summarized, and a more accurate remote sensing image classification of forest land is realized. When studying the spatial structure of landscape architecture, the indexes such as density, dispersion, mixing angle and vertical diversity have become important research contents. Through the analysis of these indicators, we can understand the spatial distribution characteristics and internal structure differences of different tree species. For example, tree species with diameter class dispersion >1 show obvious interspecific differentiation, while those with diameter class dispersion <1 are mostly young tree species. In addition, the tree species with low mixing degree often show a single tree species type, while the broad-leaved mixed forest with high mixing degree shows the diversity of tree species types and complexity of structure.

The area error evaluation indexes are all less than 20 m^2, the absolute displacement evaluation index of the center position is less than 2 degrees, and the other evaluation indexes are less than 1, which shows that the control points selected by the reference object and the segmentation object are close, the boundary shapes are basically similar, and the overall image segmentation is excellent. The accuracy test results show that the R^2 value is large, and the MRE and RMSE values are small, which shows that the analysis results are close to the real values and the fitting effect is ideal. This shows that the application of remote sensing technology in landscape architecture design has high reliability. Through the data analysis of statistical analysis software, the application value of remote sensing technology in landscape architecture planning and design is further verified. Finally, by analyzing the influence of forest structure factors on the accuracy of remote sensing classification, we can understand the classification effect and application limitations of remote sensing technology under different forest structure conditions. This provides important guidance for landscape architecture design, especially in the stands with large diameter, complex mixed degree and medium density, which can obtain more obvious layering and visual effects. Therefore, combined with the high-precision classification and segmentation results of remote sensing technology, the planning and design of landscape architecture can be carried out more effectively, and its aesthetics and functionality can be improved.

References

[1] D.U.G. Sekban and C. Acar, "Determining usages in post-mining sites according to landscape design approaches", *Land Degradation and Development*, vol. 32, no. 8, pp. 2661-2676, 2021, doi: 10.1002/ldr.3933.

[2] S.Y. Cao and X.J. Hu, "Dynamic prediction of urban landscape pattern based on remote sensing image fusion", *International Journal of Environmental Technology and Management*, vol. 24, no. 1/2, pp. 18–32, 2021, doi: 10.1504/IJETM.2021.115726.

[3] H. Zhou and Z. Dai, "Green urban garden landscape simulation platform based on high-resolution image recognition technology and GIS", *Microprocessors and Microsystems*, vol. 82, no. 4, art. no. 103893, 2021, doi: 10.1016/j.micpro.2021.103893.

[4] S.H. Lee, K.J. Han, K. Lee, K.J. Lee, and M.J. Lee, "Classification of landscape affected by deforestation using high-resolution remote sensing data and deep-learning techniques", *Remote Sensing*, vol. 12, no. 20, art. no. 3372, 2020, doi: 10.3390/rs12203372.

[5] T. Hu and W. Gong, "Urban landscape information atlas and model system based on remote sensing images", *Mobile Information Systems*, vol. 2021, art. no. 9613102, 2021, doi: 10.1155/2021/9613102.

[6] S. Liu, "Spatial distribution characteristics of urban landscape pattern based on multi-source remote sensing technology", *International Journal of Environmental Technology and Management*, vol. 24, no. 1/2, pp. 33–48, 2021, doi: 10.1504/IJETM.2021.115727.

[7] Z. Li, X. Han, L. Wang, T. Zhu, and F. Yuan, "Feature extraction and image retrieval of landscape images based on image processing", *Traitement Du Signal: Signal Image Parole*, vol. 37, no. 6, pp. 1009–1018, 2020, doi: 10.18280/ts.370613.

[8] J. Dong, H. Jiang, T. Gu, et al., "Sustainable landscape pattern: a landscape approach to serving spatial planning", *Landscape Ecology*, vol. 37 no. 1, pp. 31–42, 2022, doi: 10.1007/s10980-021-01329-0.

[9] F. Fu, S. Deng, D. Wu, W. Liu, and Z. Bai, "Research on the spatiotemporal evolution of land use landscape pattern in a county area based on CA-Markov model", *Sustainable Cities and Society*, vol. 80, art. no. 103760, 2022, doi: 10.1016/j.scs.2022.103760.

[10] B. Sowińska-Świerkosz and M. Michalik-Śnieżek, "The methodology of landscape quality (LQ) indicators analysis based on remote sensing data: Polish national parks case study", *Sustainability*, vol. 12, no. 7, pp. 1–18, 2020, doi: 10.3390/su12072810.

[11] Z.M. Miller, J. Hupy, A. Chandrasekaran, G. Shao, and S. Fei, "Application of post processing kinematic methods with UAS remote sensing in forest ecosystems", *Journal of Forestry*, vol. 119, no. 5, pp. 454–466, 2021, doi: 10.1093/jofore/fvab021.

[12] C. Mulverhill, N.C. Coops, T. Hermosilla, J.C. White, and M.A. Wulder, "Evaluating ICESat-2 for monitoring, modeling, and update of large area forest canopy height products", *Remote Sensing of Environment*, vol. 271, no. 3, art. no. 112919, 2022, doi: 10.1016/j.rse.2022.112919.

[13] F. Zhang, X. Li, et al., "Retrieval of soil salinity based on multi-source remote sensing data and differential transformation technology", *International Journal of Remote Sensing*, vol. 44, no. 3, pp. 1348–1368, 2023, doi: 10.1080/01431161.2023.2179900.

[14] Q. Tan, B. Guo, J. Hu, X. Dong, and J. Hu, "Object-oriented remote sensing image information extraction method based on multi-classifier combination and deep learning algorithm", *Pattern Recognition Letters*, vol. 141, no. 1, pp. 32–36, 2021, doi: 10.1016/j.patrec.2020.08.028.

[15] T. Ni, X. Han, B. He, X. Li, and G. Bi, "Ship detection in panchromatic optical remote sensing images based on visual saliency and multi-dimensional feature description", *Remote Sensing*, vol. 12, no. 1, art. no. 152, 2020, doi: 10.3390/rs12010152.

[16] C.A. Bouman and M. Shapiro, "A multiscale random field model for Bayesian image segmentation", *IEEE Transactions on Image Processing*, vol. 3, no. 2, pp. 162–177, 1994, doi: 10.1109/83.277898.

[17] X. Pan, C. Zhang, J. Xu, and J. Zhao, "Simplified object-based deep neural network for very high resolution remote sensing image classification", *ISPRS Journal of Photogrammetry and Remote Sensing*, vol. 181, no. 11, pp. 218–237, 2021, doi: 10.1016/j.isprsjprs.2021.09.014.

[18] A. Islam, F. Othman, Sakib N, and H.M.H. Babu, "Prevention of shoulder-surfing attack using shifting condition with the digraph substitution rules", *Artificial Intelligence and Applications*, vol. 1, no. 1, pp. 58–68, 2023, doi: 10.47852/bonviewAIA2202289.

[19] J. Margielewicz, D. Gąska, G. Litak, et al., "Influence of the configuration of elastic and dissipative elements on the energy harvesting efficiency of a tunnel effect energy harvester", *Chaos, Solitons & Fractals*, vol. 167, no. 2, art. no. 113060, 2023, doi: 10.1016/j.chaos.2022.113060.

[20] H.E. Walter, J. Pagel, H. Cooksley, et al., "Effects of biotic interactions on plant fecundity depend on spatial and functional structure of communities and time since disturbance", *Journal of Ecology*, vol. 111, no. 1, pp. 110–124, 2023, doi: 10.1111/1365-2745.14018.

[21] M.E. LeFevre, D.J. Churchill, A.J. Larson, et al., "Evaluating restoration treatment effectiveness through a comparison of residual composition, structure, and spatial pattern with historical reference sites", *Forest Science*, vol. 66, no. 5, pp. 578–588, 2020, doi: 10.1093/forsci/fxaa014.

Received: 2024-02-03, Revised: 2024-05-14